Cerebellar Degeneration in Lurcher Mice Under Confocal Laser Scanning Microscope

ZDEŇKA PURKARTOVÁ, AND FRANTIŠEK VOŽEH*
Department of Pathophysiology, Medical Faculty in Pilsen, Charles University, Lidicka 1, Pilsen, Czech Republic

KEY WORDS fluorescent double-staining; Purkinje cells; nucleus; nucleolus

ABSTRACT Lurcher mutant mice represent a natural model of genetically-determined olivocerebellar degeneration caused by a mutation in the δ2 glutamate receptor gene. They suffer from progressive postnatal loss of cerebellar Purkinje cells and a decrease of granule cells and inferior olive neurons. Their wild type littermates serve as healthy controls. A confocal laser scanning microscope was used aiming investigation the dynamics of changes in the cerebellar cortex of Lurcher and wild type mice derived from two strains during the period of 8–21 postnatal days. Fluorescent double-staining was used to visualize mainly the Purkinje cells in cerebellar slices. In wild types, only normal Purkinje cells of round or regular drop-shaped were present, when staining intensity of other individual cell structures differed in dependence on the age of the animal. In Lurcher mutants, there were still some normal-shaped cells. Nevertheless, depending on the animal's age, a wide variety of stages of the cell degeneration were depicted. The main characteristics of Purkinje cell degeneration in the early stage are: disruption of the continuity of the Purkinje cell layer, dark spots in cell nuclei and an irregular coloring of the cytoplasm. Later, the cells and their nuclei were deformed, often with two main dendrites sprouting from the cell body. Finally, the cell and nucleus margins were unclear, dendrites were significantly thickened, showing signs of shrinkage and fragmentation. Cell nucleoli underwent changes in number and appearance. No differences between the Lurcher mice of both strains (C3H and B6CBA) under examination were found. *Microsc. Res. Tech. 76:545–551, 2013.*

INTRODUCTION

The Lurcher mutant mice represent a natural model of genetically-determined olivocerebellar degeneration (Phillips, 1960). The neurodegeneration is caused by a mutation in the δ2 glutamate receptor gene (gene symbol Grid2Lc) specifically expressed by Purkinje cells (PCs) (Zuo et al., 1997). Heterozygous individual mice (+/Lc) suffer from a rapid and complete loss of the cerebellar PCs and a decrease of granule cells and inferior olive neurons number during early postnatal development. PC death has been alternatively described as necrotic (Dumesnil-Bousez and Sotelo, 1992; Dusart et al., 2006), apoptotic (Norman et al., 1995; Wüllner et al., 1995), and autophagic (Yue et al., 2002; Zanjani et al., 2009) depending on various criteria. Zuo et al. (1997) suggested that the mechanism of PC death in Lurcher mice is excitotoxic apoptosis triggered by the excessive depolarisation. Later it had been shown that while granule cells die by a purely apoptotic mechanism, the constitutive activation of Grid2 Lc induces multiple death pathways in the PCs that involve apoptosis as well as features of other mechanisms of cell death (Doughty et al., 2000). Granule cell and inferior olive neuron extinction is secondary to the target loss of their axons, the PCs. The degeneration starts at postnatal day 8 (P8). By P26 only 10% of PCs are present in the cerebellum of Lurcher mutant heterozygotes, and by P60 it is only 1%. The degeneration is complete by P90, when practically no PCs are present, and only 10% of granule cells and 30% of inferior olive neurons remain in Lurcher mutants of the C3H strain (Caddy and Biscoe, 1979). Because axons of PCs are the sole outputs from the cerebellar cortex to deep nuclei, the Lurcher mice reperesent a model of the functional decortications of the cerebellum. Nevetheless, in spite of the fact that the deep cerebellar nuclei are the primary target of the degenerating PCs axons, their neurons appear to be the only major cell type which avoids significant destruction in the Lurchers (Vogel et al., 2007). From the end of the second week of postnatal life, these mice show signs of cerebellar ataxia, higher excitability and, in addition, some of their neurons are more sensitive to a neurotoxic substance—3-acetylpyridine (Caddy and Vozeh, 1997). Heterozygous Lurcher mice further suffer from various behavioral and cognitive abnormalities (Lalonde and Thifault, 1994; Lalonde et al., 1988; Cendelín et al., 2008) including changed eyelid classical conditioning and inability to produce prepulse inhibition (Porras-Garcia et al., 2005, 2010). Mutant homozygotes (Lc/Lc) are not viable and die during intrauterine development or several days after birth. Unaffected

*Correspondence to: František Vožeh, Department of Pathophysiology, Medical Faculty in Pilsen, Charles University, Lidicka 1, 301 66 Pilsen, Czech Republic. E-mail: frantisek.vozeh@lfp.cuni.cz

Received 27 December 2012; accepted in revised form 5 February 2013

Contract grant sponsor: Charles University Research Fund (project number P36); Contract grant sponsor: Charles University; Contract grant number: SVV 266804/2013.

DOI 10.1002/jemt.22198
Published online 5 March 2013 in Wiley Online Library (wileyonlinelibrary.com).

homozygotes, wild type (+/+), are in contrast completely healthy. Lurcher mutants are successfully used for the investigation of cerebellar functions and functional and morphological consequences of the olivocerebellar degeneration. Wild type healthy littermates of these mutants serve as ideal controls (For an overview, see Vogel et al., 2007; Lalonde and Strazielle, 2007; Cendelín and Vožeh, 2013).

Classical methods as Nissl staining or Golgi-Cox impregnation complemented with electron microscope were used in the first original papers describing the quantitative changes in the cerebellar cortex and inferior olive including typical dendritic and other cellular characteristics of PCs in Lurchers (Caddy and Biscoe, 1976, 1979). Later, the use of calbindin-immunostaining which gives a Golgi-like appearance of PCs, enabled us, complemented with the electron microscope, to discover in Lurchers further valuable changes in the cells both in vivo and in vitro (Dumesnil-Bousez and Sotelo, 1992; Doughty et al., 1995; Norman et al., 1995). Despite of these excellent published works, surprisingly no microscopic study using a double fluorescent staining of the cerebellar slices was executed. Using this method we decided to clarify the role of nuclei and nucleoli changes of PCs in the dynamics of the cerebellar degeneration in the early postnatal period.

MATERIALS AND METHODS

Animals

Altogether, 56 mice aged 8–21 days (36 animals of the C3H strain–16 wild type; 20 Lurcher mutants, 20 animals of the B6CBA strain—10 wild type; 10 Lurcher mutants) of both sexes were examined. The mice were reared in standard conditions with 12:12 h light:dark cycle (6 am–6 pm), at a temperature of 22–24°C, humidity of 50%. Food and water were available ad libitum. The mice were housed in plastic cages with a metal mesh cover (18×25 cm^2, 14-cm high). Mice of both types were obtained at the Department of Pathophysiology, Faculty of Medicine in Pilsen, Charles University, by cross breeding +/+ females and +/Lc males. The experiments reported here were conducted in full compliance with the EU Guidelines for scientific experimentation on animals and with the permission of the Ethical Commision of the Faculty of Medicine in Pilsen.

Cerebellar Slices Preparation

Deeply anesthetised mice (Thiopental) were transcardially perfused with 0.07 M phosphate buffer (PBS), pH 7.4 (3–5 min) and 4% paraformaldehyde in 0.07 M phosphate buffer (PFA), pH 7.4 (15 min). Brains were isolated and post-fixed for 2 h in 4% PFA in PBS (refrigerator, 4°C). The sagital cerebellar slices (150 μm) were cut by vibratome.

Fluorescent Double-Staining

For a histological examination of the cerebella we used the fluorescent double-staining method described by Kröger and Wagner (1998). For this reason, the procedure is described here only cursorily.

The slices of the cerebellar hemisphere were incubated in LY (Lucifer Yellow CH dilithium salt, LY, Sigma L-0259), 0.2% solution in PBS for 1 h, washed for 5 min in PBS and post-fixed for 30 min in PFA. The specimens were subsequently dehydrated in 50, 70, 90, and 100% EtOH consecutively (10 min each), incubated in DiD (1,1′-dioctadecyl-3,3,3′3′-tetramethylindocarbocyanine perchlorate, Sigma 42364, 0.2% solution in EtOH) for 5 min, rinsed with 100% EtOH and rehydrated with 90% (5 min), 70% (10 min), and PBS (minimum 10 min) and coverslipped with FluorSave Reagent (Calbiochem 345789) as a aqueous mounting medium for fluorescent stained tissue sections. The slices were then observed by confocal laser scanning microscope Olympus Fluoview FV 10i.

RESULTS

The aim of this work was to investigate the postnatal dynamics of the cerebellar morphology in both Lurcher mutant and wild type mice using the fluorescent double-staining method. This procedure allowed us to describe the location, size, morphology and staining ability of the PCs. We have always described two to three pairs of mice—Lurcher and wild type—in six time periods within P8–P21. In the fluorescent double-stained sections, the cerebellar cortex layers are clearly distinguishable. Granule cells make accumulations and PCs are localized in one row between the granular and molecular layer. Cellular structures visible as green colored are hydrophilic (nucleus, nucleolus, cytoplasm), stained by Lucifer Yellow, while lipophilic structures (cell membrane, nuclear membrane, membrane organelles) stained by DiD are colored red.

Wild Type Mice

The youngest mice examined were at P8. A continual layer of PCs is clearly visible at that time and cell nuclei are sharply bound, but any outline of the cytoplasm remains unclear (Fig. 1A). Within the cell nuclei there are contours of one to three nucleoli (average number 1.40 per one cell). The dendritic tree is not yet visible.

At P9–P10 the cytoplasm has an evident green outline, round nuclei with one to three nucleoli (average number 1.33), but dendrites are not yet colored. The sequence of PCs is continuous.

At P11–P12, regular round-shaped nuclei are visible. The average number of nucleoli per nucleus remains 1.33. The cytoplasm is a brighter red color, with sharp margins (Fig. 1C). Dendrites still are not clearly visible.

At P13–P14 the morphology of cell bodies is drop-shaped, the main dendrite protrudes from the narrower pole of the cell body. Both the cell bodies and the nuclei have smooth sharp margins (Fig. 1E). In some areas, there are already visible green colored dendritic trees. The number of distinct nucleoli decreases with an average 1.30 per one nucleus at this age stage.

In older animals (P15–P21), the shape and coloring of the cell body and nucleus remain similar, but the dendritic branching is already better stained. Cell nuclei are always light green while one to two nucleoli are clearly visible (average number 1.12) as a different shade of green. Cytoplasm is usually red colored with green margins (Figs. 2A and 2C).

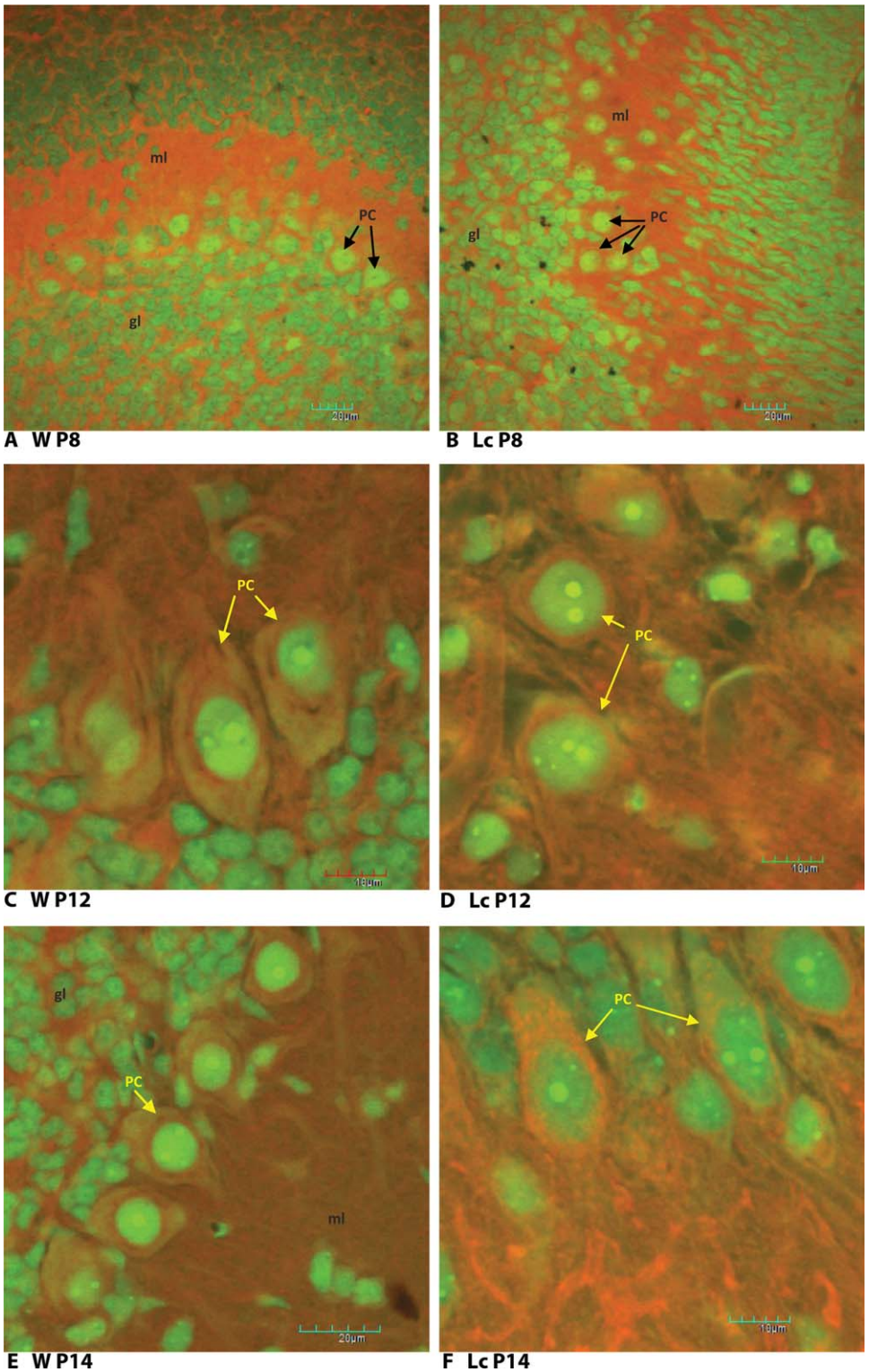

Fig. 1. **A**: Wild type mice (W) at P8. Continual layer of Purkinje cells (PCs). Granular layer (gl) is green colored, molecular layer (ml) is red colored. **B**: Lurcher mice (Lc) at P8. Disruption of the continuity of PCs monolayer. **C**: W P12. Drop-shaped cell bodies, the main dendrite protrudes from the narrower pole of the cell body. Round-shaped green nucleus with two nucleoli. **D**: Lc P12. Cytoplasm of PCs begins to be red colored, but its edges are unclear. Nucleoli are bright green colored, their number increases up to 5. **E**: W P14. The cell bodies and the nuclei have smooth sharp margins. Contours of one to three nucleoli are visible. **F**: Lc P14. PCs bodies become oval or elongated. Nucleoli are fragmented up to five to six nucleoli-like bright green objects. Cytoplasm is bright red colored. Dendrites start to be visible, they are not continuous, their surface and thickness are irregular.

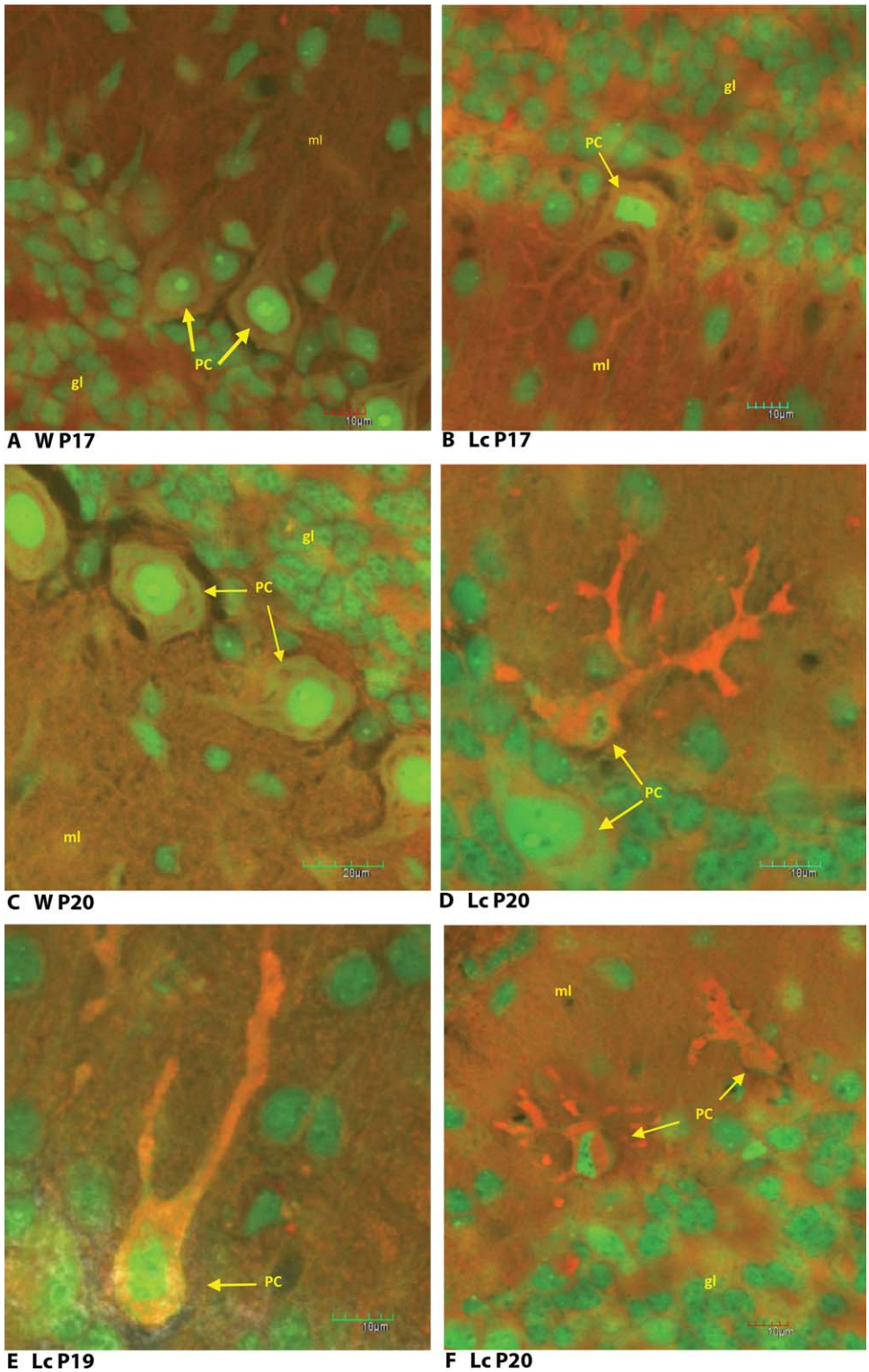

Fig. 2. **A**: W P17. The morphology of cell bodies is round or drop-shaped, the main dendrite protrudes from the narrower pole of the cell body. Both the cell bodies and the nuclei have smooth sharp margins. **B**: Lc P17. Deformed shape of the PC body and nucleus, the cell and nucleus margins are frayed. Presence of two main dendrites sprouting from the cell body. **C**: W P20. The morphology of cell bodies is round or drop-shaped, the main dendrite protrudes from the narrower pole of the cell body. Both the cell bodies and the nuclei have smooth sharp margins. Cell nuclei are always light green, one nucleolus is clearly visible as a different shade of green. **D**: Lc P20. Shrunken PC body with irregular margins. The nucleus is dark green colored with darker gray spots. Both the cytoplasm and dendrites are red colored. The cytoplasm forms only a narrow zone around the shrunk cell nucleus. The dendritic tree is thickened, showing signs of shrinkage and fragmentation. **E**: Lc P19. Deformed shape of the PC body and nucleus, nucleoli are not distinguishable, cytoplasm and two main dendrites appear to be clearly and brightly red. **F**: Lc P20. The PC body is shrunken with dark green nucleolus. Dendritic tree is not continuous, but only its chaotically arranged bright red colored fragments are visible.

Lurcher Mutants

In both strains, at P8 there are still PCs with nuclei of a round shape, but we can already identify a disruption in the continuity of their monolayer (Fig. 1B). Almost each nucleus contains one to three nucleoli of a green light-emitting color. The average number of nucleoli per nucleus is 1.60. Just like in wild types, the dendritic trees are not yet visible.

At P9–P10, the PC nuclei are still round with several dark spots in each of them. Nevertheless, the average number of their nucleoli increases to 1.70. Cytoplasm is colored irregularly and its border is usually green, and not always well marked. The continuity of the PC layer is clearly impaired.

At P11–12 many nuclei of still normal-like PCs are not spherical but have become oval or elongated. Nucleoli are bright green colored and their number increases up to 5, with an average of 2.60 (Fig. 1D). Many PCs are dislocated out of raw in their layer in direction to the molecular layer. Cytoplasm begins to be red colored but its edges are unclear. Dendritic trees are not yet visible.

In both strains, at P13–P14 there are still some normal-shaped PCs, nevertheless, also visible are the cells with signs of the next stage of degeneration. The cell and nucleus margins are frayed and their staining is not homogenous. Many darker areas appear in the nuclei, cytoplasm is bright red colored. Nucleoli are fragmented and in some cells up to five to six small bright green objects (average number per nucleus 2.70). Dendrites start to be visible, but they are not continuous and their surface and thickness are irregular. In this stage, the dendrites are usually red colored (Fig. 1F).

At P15–P18, practically all cerebellums of both strains display a wide variety of PC degeneration stages, that is, side by side there are almost normal cells, but also those in the terminal stage of the degeneration are observed there.

They are characterized by:

- abnormal, that is, deformed shape of the cell and of the nucleus with still some visible light green nucleoli-like objects or their fragments;
- a relatively frequent presence of two main dendrites sprouting from the cell body (Figs. 2B and 2E); the margins of the cell and nucleus are still saved;
- no continual layer of PCs which in spite of being still apparent.

The staining intensity of degenerating cells is typically changed. Their nuclei are lighter green colored with dark spots, while nucleoli are only sporadically distinguishable. Cytoplasm and dendrites appear to be clearly and brightly red (Fig. 2B).

In the next stage of degeneration, the ratio of nucleus and cytoplasm is changed because the latter creates only a narrow zone around the first one. The cell and nucleus margins are unclear and their staining is not homogenous. Red colored dendrites are quite visible and have thickened significantly. Some dendrites are still straight while others show signs of shrinkage and fragmentation.

At P19–P21 it is impossible to find any PC without signs of degeneration. On the border of granular and molecular layer, only seldom are PCs seen in the various stages of degeneration. Most of them show just a shrunken cell body. The cell nuclei are dark green colored with darker green spots and only in some nuclei are there still visible light green nucleoli-like objects. Moreover, the shape of nuclei is completely irregular. The red stained cytoplasm forms only a narrow irregular zone around the cell nucleus. Later, the green cell nucleus disappears and only a wrinkled red cytoplasm remains. Dendritic trees are not continuous, but only their chaotically arranged bright red colored fragments are visible. These fragments of dendrites persist even after complete cessation of the PC cell bodies (Figs. 2D–2F).

No differences were found between the examined wild type and Lurcher mice derived from both C3H and B6CBA strains that we used. There were also no differences depending on the sex of animals.

DISCUSSION

In our study, using the fluorescent double-staining method, we describe for the first time early developmental morpho-functional characteristics of PCs both in healthy animals as well as those affected by cerebellar degeneration. The study enables us to gain a new insight into the changes in these cells previously described by several authors using classical neurohistological methods as Nissl staining or Golgi-Cox (G-C) impregnation and G-C like (calbindin) procedures complemented with electron microscopy. In the double-stained cerebellar sections, the granule cell layer appears as very dense accumulations of small dark green cells, whereby axons of PCs are not evident. PC cell bodies with some visible intracellular structures are localised in one row on the border of the granular and molecular layer.

Wild Type Mice

A typical morphology of healthy PC, including the dendritic tree, is distinguishable up from P14. From P14, the PC cell bodies are approximately round or droop-shaped. Their nuclei have a round shape and they are homogenously stained. Both the cell bodies and the nuclei have smooth sharp margins. One to three nucleoli are easily distinguishable as round shaped, with an average number 1.30 (P13–14)−1.12 (P15–21). The main one dendrite protrudes from the narrower pole of the cell body. In some areas green colored dendritic trees are already visible. However, a complex richness of the dendritic branching is impossible to see as a whole in one picture. These results confirm and complete what Dumesnil-Bousez and Sotelo (1992) previously described in the calbindin immunostained sections, taken from wild type mice, that at P8 PCs dendrites have reached a phase of orientation and flattening, and from P8 to P16 they grow at first essentially in width, then exclusively in length. The dendritic arbor with a similar pattern to that of the adult is elaborated thereafter at P16. Our findings are also in agreement with those of Caddy and Biscoe (1979) that they obtained using a light microscope in cerebellar slices impregnated by G-C and also by using an electron microscope. They described in P15 wild type mouse PCs as the largest neurons in the cerebellum with the most elaborate dendritic trees in the central nervous

system and large pale nucleus containing a very electron dense nucleolus. Normal PC usually had only a single primary dendrite. In mice younger than P14, the dendritic trees are not yet evident in our double-stained slices, but the continual layer of PC cell bodies is clearly visible and cell nuclei are sharply bound with contours of one to three nucleoli. The number of nucleoli we observed in this study is also consistent with Solovei et al. (2004) that quantified the number of immunostained nucleoli of PCs in healthy C57B1/6 mice at defined days of postnatal development (P0, P2, P3, P4, P6, P14, and P21). Two, three or even four small nucleoli they found in the cerebellum of healthy newborn mice the number of which gradually decreased to 1–2 at P6. PCs of adult animals usually only had a single, very large central nucleolus. Therefore, our findings are consistent with the suggestion of Marshak et al. (1993) and Solovei et al. (2004) that the number of nucleoli can serve as a useful maturity criterion of normal healthy PCs.

Lurcher Mutants

Similarly as in wild type mice, our findings in Lurcher mice are in accordance with previous works. Nevertheless, using the double-stained fluorescent method, we obtained some new and as of yet unpublished results. Formerly several authors (Caddy and Biscoe, 1979; Dumesnil-Bousez and Sotelo, 1992; Norman et al., 1995) have corroborated that PCs of Lurcher mutants start to show morphological alternations by P8 and die during the second postnatal week. The death process is rapid and massive.

One of the earliest changes of degeneration described by Dumesnil-Bousez and Sotelo (1992), and Norman et al. (1995) is the presence of abundant varicosities along their axons. These authors suggest that the varicosities, present in calbindin-immunostained slices already at P8, arise as a consequence of an impaired axoplasmatic transport related to metabolic changes in PCs. In the electron-microscopic pictures of the cerebellar slices from Lurcher mice at P15 these axonal swellings were already described also by Caddy and Biscoe (1979). As already mentioned, in the fluorescent double-stained sections we were unable to distinguish the axons, because they were covered with clusters of granule cells. Nevertheless, one of the other constants observed in the electron microscope in Lurchers at P8—clumps of chromatin, preferentially located against the inner surface of the nuclear membrane—described also by Caddy and Biscoe (1979) and Dumesnil-Bousez and Sotelo, (1992) were found as well. They fully correspond to our findings of several dark spots clearly visible in each PC nucleus from P9 to P10 and later on. We also confirmed further typical findings in Lurchers described by Dumesnil-Bousez and Sotelo (1992), that is, ectopic PC somata, visible in the deeper half of the molecular layer in the calbidin-immunostained sections from P10. In our observations, we saw such dislocated PCs in the direction to the molecular layer somewhat later from P11 on and the continuity of the PC layer was evidently impaired.

At P12 and later, the PCs often exhibit multiple primary dendrites. These dendrites develop a thick and deformed appearance (Dumesnil-Bousez and Sotelo, 1992). Nevertheless, the dendritic trees of these cells in Lurchers are obviously smaller (Caddy and Biscoe, 1979).

The abnormalities of the PC dendritic trees at P8–P13 are not yet evaluable. It is similar to that of healthy mice when dendritic trees are seen up from P13–P14. At this postnatal time period the cytoplasm and dendrites begin to be color red, that is, lipophilic. These findings undoubtedly correspond with a greater proportion of lipid droplets in both PC somata and dendrites as previously reported (Caddy and Biscoe, 1979; Dumesnil-Bousez and Sotelo, 1992; Norman et al., 1995) indicating irreversible signs of necrosis together with increasing number of lysosomes, altered mitochondria and vacuoles. However, up to P15 we could find in our observations quite normal PCs among many abnormal ones in various stages of the degeneration. In the advanced stage of the degeneration, the ratio of nucleus and cytoplasm has undergone change. There is only a narrow zone of cytoplasm. The cell and nucleus margins are frayed and their staining is not more homogenous. Dendrites are quite well visible and significantly thickened. Some dendrites are still straight while others show signs of shrinkage and fragmentation.

At P19–P21, we cannot find in Lurchers any cells without signs of degeneration. Instead of a cell layer there are only solitary PCs. Most of them show a shrunken cell body. Cell nuclei are dark green with darker green spots, in some nuclei light green nucleoli-like objects or their fragments are still visible. The shape of nuclei is completely irregular. The red colored cytoplasm forms only a narrow irregular zone around the cell nucleus. Later, a green cell nucleus disappears and only a wrinkled red cytoplasm remains. The dendritic tree is not continual any more, because of resulting in its chaotically arranged fragments, still colored bright red. Fragments of dendrites persist even after complete cessation of PC cell body.

Completely new in our investigation of the cerebellar degeneration in Lurchers and in a sharp contrast to the normal development of PC in wild type mice are the dynamic changes of nucleoli in their number and appearance.

In contrast with wild types with an average number of nucleoli per one cell 1.40 at P8, we found a higher amount of them with an average 1.60 at the same postnatal age in Lurchers. Moreover, in the next stages under observation, we discovered the opposite trend in the PCs nucleoli development. Although in the wild type mice the number of nucleoli gradually decreased (with average 1.12 at P15–P21), in Lurchers it increased at the same time with an average 2.70 of smaller nucleoli-like objects. At P18–P21 there were practically no such objects visible any more. While our findings concerning the number of nucleoli in wild types are fully in agreement with those in ICR mice of Marshak et al. (1993) and in C57BL/6 mice of Solovei et al. (2004), in Lurchers such a study has not yet been performed. Nevertheless, our findings correspond to a considerable extent with results of Baltanás et al. (2010) described in their immunofluorescent and ultrastructural study. There they observed nucleolar fragmentation and disruption in pcd mice (derived from C57BL/6J strain—males and DBA/2J-females) at P20. Despite a completely different genetical background of the PC degeneration in these mice, the consequences

of a complete loss of PCs and early progressive ataxia are similar to those in Lurchers. A hypothesis which the authors offer as an explanation to the decomposition of the nucleoli and also Cajal bodies in the pcd mice suggests that the changes are early and are sensitive nuclear hallmarks of DNA damage-induced neuronal degeneration in PCs and, presumably, in other neurons. Another theory explaining nuclear processes connected with cerebellar ataxias proposed by Lim et al. (2006) stresses the global transcriptional activity, nuclear pre-mRNA processing and abnormalities of the ataxia protein network which might cause nucleolar alteration without the involvement of any DNA damage. Therefore, our findings of primarily a higher number of nucleoli, their real or seeming multiplication followed by fragmentation are undoubtedly signs of nuclear degeneration of PCs in Lurchers. To what extent DNA-damaging processes, abnormal ataxia protein network or some other mechanisms are involved is still an open question and due attention will be paid to it in the future. On the contrary, what we can state with certainty is that there were not any different impacts in the described characteristics of the cerebellar degeneration in Lurcher mice of either of the C3H and B6CBA strains under examination. Also, no differences were found in relation to sex of animals.

ACKNOWLEDGMENT

The authors like to express their thanks to Mr. Christopher Koy, Ph.D. for proofreading the text.

REFERENCES

Baltanás FC, Casafont I, Weruaga E, Alonso JR, Berciano MT, Lafarga M. 2010. Nucleolar disruption and Cajal body disassembly are nuclear hallmarks of DNA damage-induced neurodegeneration in Purkinje cells. Brain Pathol 21:374–88.

Caddy KWT, Biscoe TJ. 1979. Structural and quantitative studies on the normal C3H and Lurcher mutant mouse. Philos Trans R Soc Lond B Biol Sci 287:167–201.

Caddy KWT, Vožeh F. 1997. The effect of 3-acetylpyridine on olivary neuron degeneration in Lurcher mutant and wild type mice. Eur J Pharmacol 330:139–142.

Cendelín J, Korelusova I, Vožeh F. 2008. The effect of repeated rotarod training on motor skills and spatial learning ability in Lurcher mutant mice. Behav Brain Res 189:65–74.

Cendelín J, Vožeh F. 2013. Lurcher mouse. In: Manto M, Gruol DL, Schmahmann JD, Koibuchi N, Rossi F, editors. Handbook of the cerebellum and cerebellar disorders. Springer Verlag, New York. pp. 1499–1520.

Doughty ML, De Jager PL, Korsmeyer SJ, Heintz N. 2000. Neurodegeneration in Lurcher mice occurs via multiple cell death pathways. J Neurosci 20:3687–3694.

Doughty ML, Patterson L, Caddy KW. 1995. Cerebellar Purkinje cells from the Lurcher mutant and wild-type mouse grown in vitro: a light and electron microscope study. J Comp Neurol 19:161–179.

Dumesnil-Bousez N, Sotelo C. 1992. Early development of the Lurcher cerebellum: Purkinje cell alterations and impairment of synaptogenesis. J Neurocytol 21:506–529.

Dusart I, Guenet JL, Sotelo C. 2006. Purkinje cell death: Differences between developmental cell death and neurodegenerative death in mutant mice. Cerebellum 5:163–173.

Kröger RHH, Wagner H-J. 1998. A fluorescent double stain for visualization of neural tissue by confocal laser scanning microscopy. J Neurosci Methods 84:87–92.

Lalonde R, Lamarre Y, Smith AM. 1988. Does the mutant mouse lurcher have deficits in spatially oriented behaviours. Brain Res 455:24–30.

Lalonde R, Strazielle C. 2007. Spontaneous and induced mouse mutations with cerebellar dysfunctions: Behavior and neurochemistry. Brain Res 1140:51–74.

Lalonde R, Thifault S. 1994. Absence of an association between motor coordination and spatial orientation in lurcher mutant mice. Behav Genet 24:497–501.

Lim J, Hao T, Shaw C, Patel AJ, Szabó G, Rual JF, Fisk CJ, Li N, Smolyar A, Hill DE, Barabási Al, Vidal M, Zoghbi HY. 2006. A protein-protein interaction network for human inherited ataxias and disorders of Purkinje cell degeneration. Cell 125:801–814.

Marshak TL, Mares V, Pavlik A. 1993. The effect of methylazoxymethanol on neuronal differentiation in the murine cerebellum. Ontogenez 24:62–9.

Norman DJ, Feng L, Cheng SS, Gubbay J, Chan E, Heintz N. 1995. The lurcher gene induces apoptotic death in cerebellar Purkinje cells. Development 121:1183–1193.

Phillips RJS. 1960. "Lurcher", new gene in linkage group XI of the house mouse. J Genet 57:35–42.

Porras-Garcia E, Cendelin J, Dominiguez-del-Toro E, Vozeh F, Delgado-Garcia JM. 2005. Purkinje cell loss affects differentially the execution, acquisition and prepulse inhibition of skeletal and facial motor responses in Lurcher mice. Eur J Neurosci 21:979–988.

Porras-Garcia E, Sanches-Campusano R, Martines-Vargas D, Dominiguez-del-Toro E, Cendelin J, Vozeh F, Delgado-Garcia JM. 2010. Behavioral characteristics, associative learning capabilities, and dynamic association mapping in an animal model of cerebellar degeneration. J Neurophysiol 104:346–365.

Solovei I, Grandi N, Knoth R, Volk B, Cremer T. 2004. Positional changes of pericentromeric heterochromatin and nucleoli in postmitotic Purkinje cells during murine cerebellum development. Cytogenet Genome Res 105:302–310.

Vogel MW, Caston J, Yuzaki M, Mariani J. 2007. The Lurcher mouse: Fresh insights from an old mutant. Brain Res 1140:4–18.

Wüllner U, Löschmann PA, Weller M, Klockgether T. 1995. Apoptotic cell death in the cerebellum of mutant weaver and lurcher mice. Neurosci Lett 200:109–112.

Yue Z, Horton A, Bravin M, DeJager PL, Selimi F, Heintz N. 2002. A novel protein complex linking the δ2 glutamate receptor and autophagy: Implications for neurodegeneration in Lurcher mice. Neuron 35:921–933.

Zanjani HS, McFarland R, Cavelier P, Blokhin A, Gautheron V, Levenes C, Bambrick LL, Mariani J, Vogel MW. 2009. Death and survival of heterozygous Lurcher Purkinje cells in vitro. Dev Neurobiol 69:505–517.

Zuo J, De Jager PL, Takahasi KJ, Jiang W, Linden DJ, Heintz N. 1997. Neurodegeneration in Lurcher mice caused by mutation of delta2 glutamate receptor gene. Nature 388:769–773.